

## AT622 Section 4

### Elementary Radiative Transfer

The aim of this section is to acquaint students with simple, basic concepts of radiative transfer as it applies to both a sourceless atmosphere and an atmosphere that contains general or arbitrary sources of radiation. The equation derived will be applied to study radiative transfer in an absorbing atmosphere in the context of infrared transfer in a clear atmosphere. Thus we begin to learn how these transfer processes shape the thermal structure of the atmosphere.

#### 4.1 Extinction

The propagation of radiation through attenuating material undergoes changes as a result of radiative processes that take place in the medium. Extinction is one of the elementary processes affecting this transfer and it is defined as follows. The change in intensity  $dI_v$  on propagating along a path of length  $ds$  (Fig. 4.1) is empirically related to the incident intensity of the radiation via *Lambert's law of extinction*

$$dI_v = -\sigma_{ext} I_v ds \quad (4.1)$$

where  $\sigma_{ext}$  is the proportionality constant known as the extinction coefficient. This extinction may occur as a result of scattering by particles or molecules in the atmosphere, by absorption by particles and molecules in the atmosphere or by a combination of both (although the molecules that scatter radiation are, on the whole, different from the molecules that absorb radiation—The reason for this will become apparent later). Thus we can write

$$\sigma_{ext} = \sigma_{sca} + \sigma_{abs}$$

where examination of Eqn. (4.1) reveals that the quantity

$$d\tau = \sigma_{ext} ds$$

is unitless. This is a fundamental quantity known as the *optical path* and when the path is vertical, it is the *optical depth*. We will see later that there are different ways of measuring  $\sigma_{ext}$  and thus different complementary measures of path length  $ds$ .

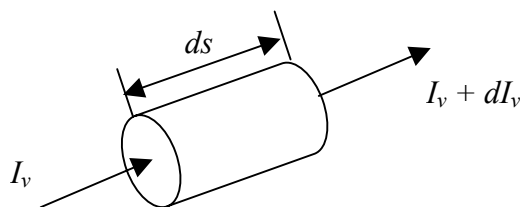


Fig. 4.1 The law of extinction.

Equation (4.1) may be readily cast into a radiative transfer equation

$$\frac{dI_v}{ds} = -\sigma_{ext,v} I_v, \quad (4.2)$$

which has a solution of the form

$$I_v(s'') = I_v(s') \exp(-\tau_v), \quad (4.3)$$

where  $\tau_v = \int_{s'}^{s''} \sigma_{ext,v}(s) ds$  is the optical thickness. This solution, referred to as *Beer's law*, serves as the basis for many remote sensing applications and is a good approximation to the measurements of sunlight in the clear and relatively clean atmosphere. For example, consider the measurement of direct sunlight. If the sun is inclined at an angle  $\theta_\odot$  from the vertical (the solar zenith angle), then Eqn. (4.3) becomes

$$I_v(\tau_v^*) = I_v(\tau_v = 0) \exp(-\tau_v^* / \cos \theta_\odot), \quad (4.4)$$

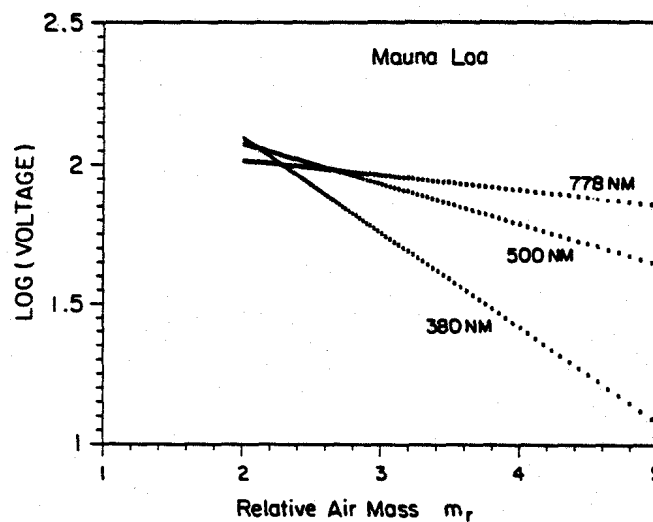


Fig. 4.2 An example of a Lambertian plot: the logarithm of solar intensity is plotted as a function of optical air mass for clear, stable atmospheric conditions.

where  $\tau_v^*$  is the optical depth. The logarithmic form of Eqn. (4.4) is

$$\ln I_v(\tau_v^*) = \ln I_v(\tau_v = 0) - \tau_v^* / \cos \theta_\odot. \quad (4.5)$$

Figure 4.2 is an example of this type of relationship derived from radiometer (pyrheliometer) measurements obtained at the Manua Loa Observatory. The data are from a spectral radiometer pointed towards the sun and measurements are recorded as the sun moves across the sky throughout the course of a day. If the logarithms of these measured intensities are plotted as a function of  $\sec \theta_\odot$  then the optical depth  $\tau_v^*$  is the slope of the line and the incident intensity  $I_v(\tau_\lambda = 0)$  is given by the intercept determined by extrapolating  $\sec \theta_\odot$  to zero. From this diagram we see how the clear sky measurements of solar fluxes at the wavelengths of the filters used is very closely represented by Lamberts law.

**Example 4.1** Extinction—it's black and white.

The experimenter who observes that extinction has taken place by measuring radiation at two levels in the atmosphere cannot determine if the radiation is decreased because it is absorbed or decreased because it is scattered. A simple illustration of this elementary point is well described by Bohren (1987) and is highlighted in Fig. 4.3. One cannot distinguish between the images of two water-filled glass petri dishes projected on a screen yet their darkness arises from different mechanisms. Light incident on the inky water is attenuated mainly by absorption, whereas light incident on the milky water is mostly scattered. It is only by looking at the dishes that this difference between them becomes apparent. An important scattering parameter that helps quantify these differences is the *single scattering albedo*  $\tilde{\omega}_o$ . This parameter is the ratio of the amount of scattering that attenuates the light to the total extinction (absorption *plus* scattering). For the milky water we might infer that  $\tilde{\omega}_o \approx 1$  since light is primarily scattered in all directions from the dish. On the other hand,  $\tilde{\omega}_o \approx 0$  for inky water as little light is scattered and most of the extinction occurs through absorption. We will see later how the parameter  $\tilde{\omega}_o$  is fundamental to problems of multiple scattering and thus for understanding how radiation is transferred from layer to layer in clouds.

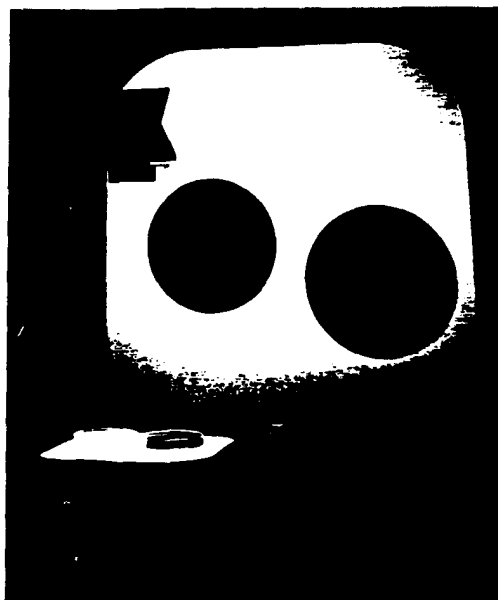


*Fig. 4.3. The images of two water-filled glass beakers projected on a screen are identical yet their darkness (extinction) arises from different mechanisms. Light incident on the inky water is attenuated mainly by absorption, whereas light incident on the milky water is attenuated mostly by scattering. It is only by looking at the beakers that this difference becomes apparent.*

## 4.2 Adding Sources of Radiation

Example 4.1 illustrates how multiple scattering confuses the interactions between radiation and the atmosphere. For example, photons originally scattered away from the viewing direction can reappear, and scattering can also cause photons to arrive having been incident from some other direction. Multiple scattering acts as a kind of source of radiation (this is sometimes referred to as virtual emission).

Whether it is real emission (governed by Kirchoff's law, chapter 1) or virtual emission that contributes to a beam as it traverses a path of length  $ds$ , the increased intensity may be expressed as

$$x dI_v = \sigma_{ext,v} J_v ds, \quad (4.6)$$

which defines the *source function*  $J_v$ . When this emission takes place in the lower atmosphere where thermodynamic equilibrium occurs,  $J_v = B_v$ .

The net change in radiation along a path element,  $ds$ , due to the combination of emission and extinction is

$$dI_\lambda = dI_\lambda(\text{emission}) + dI_\lambda(\text{extinction}). \quad (4.7)$$

and with the combination of Eqns. (4.6) and (4.1) we obtain

$$\frac{dI_v}{ds} = -\sigma_{ext,v} [I_v - J_v], \quad (4.8a)$$

## 4.3 A Radiative Transfer Equation for Absorption/Emission

In many problems of infrared radiative transfer that interest the atmospheric scientist it is reasonable to neglect scattering so we can substitute  $\sigma_{abs}$  for  $\sigma_{ext}$ . Then substituting Eqns. (4.1) and (4.6) in Eqn. (4.7), we obtain the following transfer equation

$$\frac{dI_v}{ds} = -\sigma_{abs,v} [I_v - B_v], \quad (4.8b)$$

which is the mathematical relationship describing how radiation is transferred from one layer to another layer as a result of absorption and emission. The amount of radiation leaving the end of the path is a function of the distribution of absorber along the path (we will see that this is implied in  $\sigma_{abs,v}$ ) and the distribution of temperature (through the presence  $B_v$ ).

In general, the interactions between radiation and the gases of the atmosphere are weak enough that the photon mean free path exceeds the mean free path of molecules. Hence, the radiative transfer in the atmosphere tends to be nonlocal requiring integration of processes along the path. To derive this integral form of the radiative transfer equation, we first make use of the definition,  $d\tau_v(s) = -\sigma_{abs,v}(s) ds$ , for an element of the optical thickness (the reason for the negative sign in this definition of optical thickness becomes evident below) and then multiply each side of Eqn. (4.8b) by the factor  $\exp(-\tau_v(s))$ . Combining terms, we obtain

$$\frac{dI_{\nu} e^{-\tau_{\nu}(s)}}{d\tau_{\nu}} = -B_{\nu} e^{-\tau_{\nu}(s)}. \quad (4.9)$$

Consider a general path extending from some point  $s = s'$  to an end point  $s = s''$ . Then simple integration of Eqn. (4.9) from  $s'$  to  $s''$  yields

$$I_{\nu}(s'')e^{-\tau_{\nu}(s'')} - I_{\nu}(s')e^{-\tau_{\nu}(s')} = \int_{\tau(s'')}^{\tau(s')} B_{\nu}(s)e^{-\tau_{\nu}(s)} d\tau(s)$$

which, on rearrangement, gives

$$I(s'') = I(s')e^{-[\tau(s'')-\tau(s')]} + \int_{s'}^{s''} B(s)e^{-[\tau(s)-\tau(s'')]} d\tau(s) \quad (4.10)$$

where the frequency dependence of all factors (we could have equally used wavelength rather than frequency here) in Eqn. (4.10) is taken to be understood. The first term on the right hand side of this equation represents the radiation, originally incident at  $s'$ , that is transmitted to  $s''$ . We will refer to this as the surface term. The integral term represents the emitted radiation that accumulates along the path and transmitted to  $s''$ .

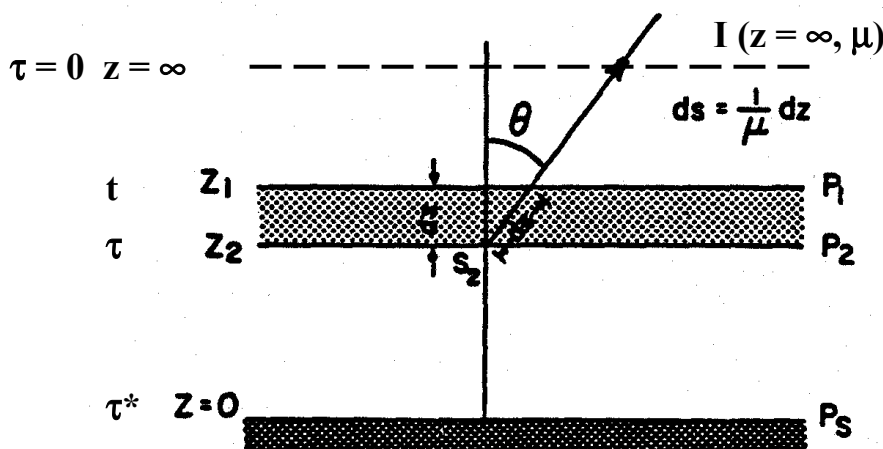


Fig. 4.4 The geometric setting for the integral transfer equation in a plane parallel vertically stratified atmosphere.

When Eqn. (4.10) is applied to the atmosphere, Fig. 4.4, it is customary, but not necessarily realistic, to assume that the atmosphere is plane parallel and horizontally homogeneous. For such a stratified atmosphere, the integral equation can be expressed in terms of optical depth  $\tau(z)$  (rather than optical thickness  $\tau(s)$ ). It is conventional to define the optical depth such that  $\tau = 0$  at the top of the atmosphere and  $\tau = \tau^*$  at the surface.<sup>1</sup> For slant paths, the expression relating optical depth to optical path is

$$\tau(s) = \tau(z)/\cos \theta.$$

<sup>1</sup> The convention that  $\tau$  increases downward from the top of the atmosphere has roots in the traditional astrophysics literature on radiative transfer where  $\tau$  is taken to increase along the direction of sunlight entering the atmosphere. Optical depth increases in the opposite sense to  $z$  and hence the negative sign in its definition.

producing

$$I(\tau, +\mu) = I(\tau^*, -\mu)e^{-(\tau^* - \tau)/\mu} + \int_{\tau}^{\tau^*} B(t)e^{-(t - \tau)/\mu} \frac{dt}{\mu} \quad (4.11a)$$

for  $0 < \mu < 1$ , which defines radiation that upwells from the atmosphere, and

$$I(\tau, -\mu) = I(0, -\mu)e^{-\tau/|\mu|} + \int_0^{\tau} B(t)e^{-(\tau - t)/|\mu|} \frac{dt}{|\mu|} \quad (4.11b)$$

for  $0 > \mu > -1$  for downwelling radiation.

Figure 4.5 is an example of a measured intensity spectrum obtained from an interferometer instrument flown on Nimbus 4. Superimposed on the measurements are the black body curves for selected temperatures. Also highlighted are spectral positions of the absorption bands of the predominant absorbing gases. This diagram more clearly shows how emissions from different levels in the atmosphere (and therefore at different temperatures) combine to produce the observed spectra. For instance, emission in the central portions of the 9.6  $\mu\text{m}$  ozone band occurs at temperatures below about 250°K, and emission in the 15  $\mu\text{m}$  CO<sub>2</sub> band varies throughout the atmosphere according to the spectral position relative to the band center. For both O<sub>3</sub> and CO<sub>2</sub>, the increase in emitted radiation in the strongest part of the center of the absorption band occurs higher up in the atmosphere than in the neighboring spectral regions and is an indication of the increase in temperature with increasing altitude in the stratosphere. Also noteworthy is the water vapor emission that is confined to the lower atmosphere (emission by the vibration and rotation bands is broadly characterized by the 275°K black body curve for this example). An important spectral region is the atmospheric window between about 800  $\text{cm}^{-1}$  and 1200  $\text{cm}^{-1}$  in which the atmosphere is almost transparent (except for the ozone band) and the emission originates from levels close to the surface.

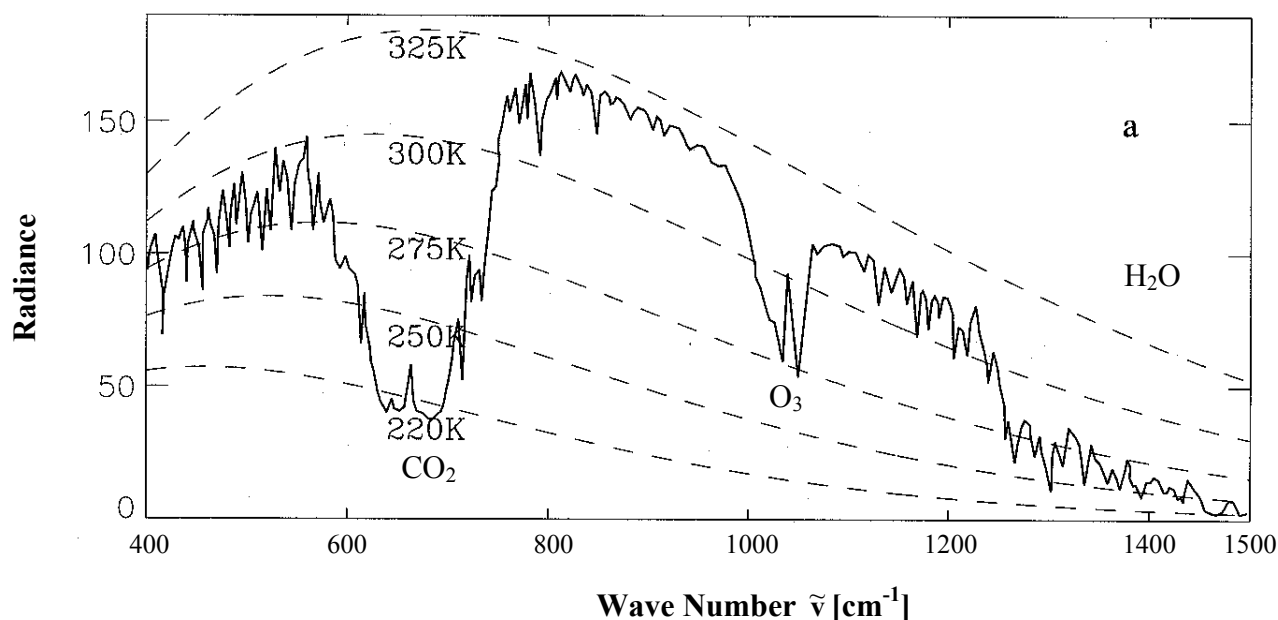


Fig. 4.5 Earth's emission spectrum seen at the top of the atmosphere.

**Example 4.2: Radiative transfer in an isothermal atmosphere**

Consider a simple demonstration of Eqn. (4.11): Isothermal atmosphere

- an isothermal atmosphere,  $B(t) = B$ . Thus

$$I(\tau^*, \mu) = B(1 - e^{-\tau^*/\mu}).$$

This leads to limb brightening for downwelling radiation at  $\tau = \tau^*$  and isotropic fields for the upwelling intensity at  $\tau = 0$  since

$$I(0, \mu) = B e^{-\tau^*/\mu} + B(1 - e^{-\tau^*/\mu}) = B.$$

- For the nonisothermal problem, the solutions for the intensities and fluxes become much more complex. For illustrative purposes, assume the Planck function to be linear in optical depth. Let  $B_o$  and  $B^*$  be the Planck functions at the top ( $\tau = 0$ ) and bottom of the atmosphere, respectively. It is easily shown that

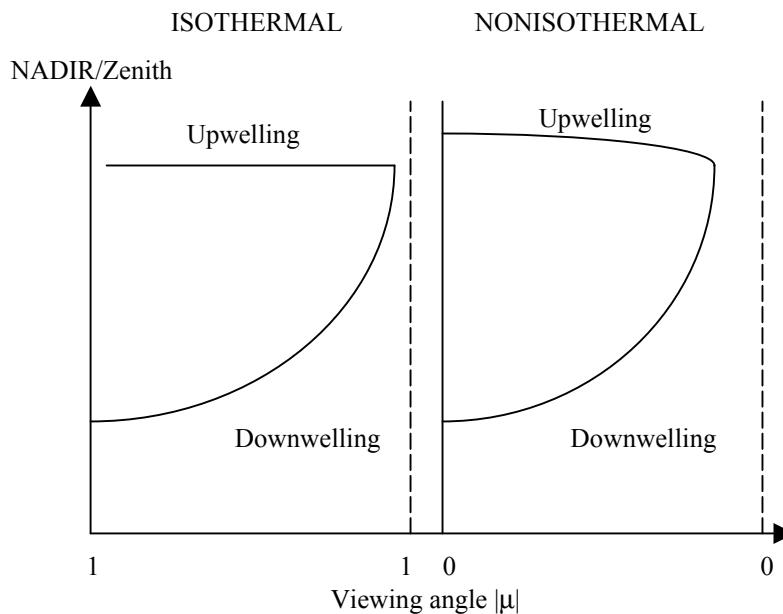
$$I(\tau^*, \mu) = B_o(1 - e^{-\tau^*/\mu}) + (B^* - B_o) \left( 1 - \frac{\mu}{\tau^*} (1 - e^{-\tau^*/\mu}) \right)$$

(Limb Brightening)

$$I(0, \mu) = B^* e^{-\tau^*/\mu} + B^* (1 - e^{-\tau^*/\mu}) - (B^* - B_o)(1 - e^{-\tau^*/\mu})$$

(Limb Darkening)

when  $B(\tau) = B_o + (B^* - B_o)\tau/\tau^*$ . Generally the angular variation of upwelled radiation is less marked than that of downwelled radiation.



Examples of the angular variation of upwelling and downwelling emitted radiation.

**Example 4.3:** The exponential integral, flux equation and diffusivity

We adopt the transfer equations above to obtain fluxes. We choose to demonstrate this using Eqn. (4.11a), which is integrated as follows:

$$2\pi \int_0^1 I(\tau, +\mu) \mu d\mu = 2\pi \int_0^1 I(\tau^*, \mu) e^{-(\tau^*-\tau)/\mu} \mu d\mu + 2\pi \int_0^1 d\mu \int_{\tau}^{\tau^*} B(t) e^{-(t-\tau)/\mu} dt$$

which becomes

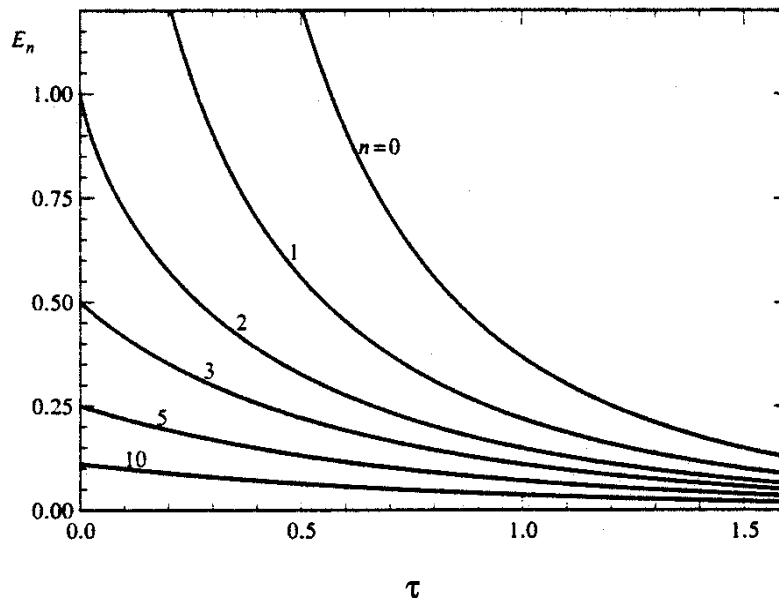
$$F^+(\tau) = \pi I_s \int_0^1 e^{-(\tau^*-\tau)/\mu} \mu d\mu + 2 \int_{\tau}^{\tau^*} \pi B(t) \int_0^1 e^{-(t-\tau)/\mu} d\mu dt$$

where the surface radiation is taken to be isotropic. Introducing the exponential integral function

$$E_n(x) = \int_1^{\infty} \frac{e^{-xt}}{t^n} dt = \int_0^1 \mu^{n-2} e^{-x/\mu} d\mu$$

then the flux equation becomes

$$F^+(\tau) = \pi I_s 2E_3(\tau^*-\tau) + 2 \int_{\tau}^{\tau^*} \pi B(t) E_2(t-\tau) dt$$



General behavior of the exponential integral. Shows also that  $2E_3(x) \approx \exp(-\beta x)$  where  $\beta = 1.66$  and is known as the diffusivity factor. We return to this factor and its interpretation later but note that it represents a transmission function for flux.

#### 4.4 Gray Body Transfer: The Role of Radiation on the Temperature Structure of the Atmosphere

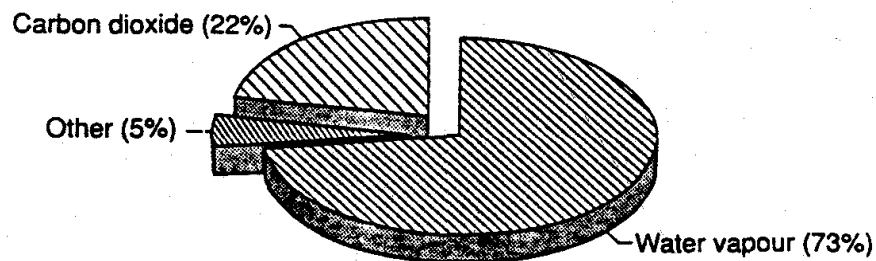
It is instructive to study the role of infrared radiation in a simple climate model, in which the rather drastic assumption is made that the optical depth is independent of frequency. This is known as the “gray” approximation. To this end, we will consider the concept of gray body radiative transfer and further introduce the notion of radiative equilibrium—a notion that we will return to later.

##### Example 4.4: An estimate of the gray-body optical depth

The spectral optical depth is a complex function of wavelength and several ways of spectrally averaging  $\tau$  exist. The approach used here is one appropriate to the radiative equilibrium arguments introduced to arrive at Eqn. (4.17) and follows from the following flux-mean mass absorption coefficient (Mihalas, 1978)

$$k_f = F_\infty^{-1} \int k_f F_{\infty, \lambda} d\lambda.$$

The contribution to  $\tau$  by water vapor, carbon dioxide and other minor greenhouse gases present in the Earth's atmosphere obtained using  $k_f$  in Eqn. (4.13), is shown below. The spectral absorption data used to derive  $k_f$  are those tabulated by Rothman (1981). The total gray body optical depth derived from these data is  $\tau = 3.9$  corresponding to  $w = 28 \text{ kgm}^{-2}$ , which is close to the global mean values of  $w$ . The value  $\tau = 3.9$  is larger than the value of the optical depth derived from later considerations. This highlights the ambiguity of the quantitative meaning of  $\tau$  and to understand the value it is necessary to understand how it is derived. The advantage of the flux-weighted value is that it allows us to estimate  $\tau$  from spectral integration and thus the contributions by individual gases. These contributions clearly emphasize the dominance of water vapor to the total gray body optical depth for the global mean conditions considered.



A pie diagram showing the percentage of the gray body optical depth due to water vapor and other greenhouse gases in the Earth's atmosphere based on typical mean global concentrations of these gases.

In dealing with gray body transfer, let us begin with a monochromatic RTE

$$\mu \frac{dI(\tau, \mu)}{d\tau} = I(\tau, \mu) - B(T) \quad (4.12a)$$

$$-\mu \frac{dI(\tau, -\mu)}{d\tau} = I(\tau, -\mu) - B(T) \quad (4.12b)$$

where  $I$  is the intensity,  $\mu = \cos \theta$  where  $\theta$  is the angle of the beam from the zenith. The optical depth is defined as

$$\tau = \int_z^\infty k \rho_a dz \quad (4.13)$$

where  $k$  is the mass absorption coefficient,  $\rho_a$  is the density of the absorbing gas, and  $z$  is the lowest end point of the path. It is simple to cast these equations into equations for (see box below) upward ( $F^+$ ) and downward ( $F^-$ ) hemispheric fluxes,

$$\frac{dF^+}{d\tilde{\tau}} = F^+ - \pi B, \quad (4.14a)$$

$$-\frac{dF^-}{d\tilde{\tau}} = F^- - \pi B, \quad (4.14b)$$

where

$$\tilde{\tau} = \frac{3}{2} \tau.$$

We now introduce the gray body assumption, which means if we take  $\tilde{\tau}$  to be independent of wavelength (we know that it is not), then we can treat the fluxes in Eqns. (4.14a and b) as broadband quantities and replace  $\pi B$  with  $\sigma T^4$ . The factor of 3/2 is a form of *diffusivity factor* and its interpretation follows from the considerations discussed below.

Let us introduce the notion of radiative equilibrium, which for our purpose means that at the top of the atmosphere

$$F^+(\tilde{\tau} = 0) = \frac{Q_\odot}{4}(1 - \alpha) = F_\infty \quad (4.15a)$$

where  $Q_\odot$  is the global-annual mean incoming solar radiation at the top of the atmosphere and  $\alpha$  is the planetary albedo (**note:** these are all broadband quantities). Radiative equilibrium also implies that throughout the atmosphere (why??)

$$F_{net} = F^+(\tilde{\tau}) - F^-(\tilde{\tau}) = const \quad (4.15b)$$

(we are also assuming that no solar radiation is absorbed in the atmosphere). Given this condition, it follows from Eqn. (4.14a) that

$$F^+(\tilde{\tau}) + F^-(\tilde{\tau}) = 2\pi B(\tilde{\tau})$$

and further from (4.15b) that

$$F^+(\tilde{\tau}) + F^-(\tilde{\tau}) = F_{net} \tilde{\tau} + C.$$

On combining these equations we obtain

$$B(\tilde{\tau}) = \frac{F_{net}}{2\pi} (\tilde{\tau} + 1).$$

**Example 4.5:** A further derivation of the flux equations

It is a relatively simple matter to convert Eqns. (4.12a and b) into flux equations if we define a direction  $\bar{\mu}$  such that the flux

$$F^+ = 2\pi \int_0^+ I(\mu) \mu d\mu = \pi I(\bar{\mu}).$$

Thus it is straightforward to write down the RTE at  $\mu = \bar{\mu}$  and by multiplying each side of this equation by a factor of  $\pi$  we arrive at Eqns. (4.14a and b) with  $\bar{\mu} = 2/3$ .

The solution to these equations follows by first differencing these equations to yield

$$\frac{dF_{net}}{d\tilde{\tau}} = (F^+ + F^-) - 2\pi B \quad (4.15a)$$

(remember  $F_{net} = (F^+ - F^-)$ ) and summing the equations to obtain

$$\frac{d(F^+ + F^-)}{d\tilde{\tau}} = F_{net} \quad (4.15b)$$

which provides two equations for the two unknowns  $F_{net}$  and  $(F^+ + F^-)$ . We will now explore these solutions given an additional assumption about radiative equilibrium.

At the top of the atmosphere, we have  $\tilde{\tau} = 0$  and  $F^- = 0$ , so that  $F_{net} = F_\infty$  and  $C = F_{net}$ . Further, under the gray body assumption

$$\sigma T^4(\tilde{\tau}) = \frac{F_\infty}{2} (\tilde{\tau} + 1) \quad (4.16a)$$

At the bottom of the atmosphere, where  $\tilde{\tau} = \tilde{\tau}_s$ , we have  $F^+ = \sigma T_s^4$  and it follows that

$$\sigma T_s^4 - F^-(\tilde{\tau}_s) = F_\infty$$

$$\sigma T_s^4 + F^-(\tilde{\tau}_s) = F_\infty (\tilde{\tau}_s + 1)$$

and that

$$\sigma T_s^4 = \frac{F_\infty}{2} [2 + \tilde{\tau}_s] \quad (4.16b)$$

$$F_g^- = F^-(\tilde{\tau}_s) = \frac{F_\infty}{2} \tilde{\tau}_s \quad (4.16c)$$

at the surface.

**Example 4.6: Skin temperatures and temperature discontinuities**

The solutions represented by Eqns. (4.16a) and (4.16b) provide rather interesting insights into the temperature profiles that are predicted by these equations. One of the results of this model is an estimate of the 'skin' temperature, which we think of as a measure of the stratospheric temperature. We obtain this using Eqn. (4.16a) with  $\tilde{\tau} = 0$

$$\sigma T^4(\tilde{\tau} = 0) = \frac{F_\infty}{2}$$

and with  $F_\infty \approx 235 \text{ Wm}^{-2}$ , it follows that this temperature is  $T_{skin} = [117.5/5.68 \times 10^{-8}]^{0.25} = 213 \text{ K}$ .

The solutions in Eqns. (4.16a) and (4.16b) predict a discontinuity between the surface temperature  $T_s$  and the air temperature just above the ground  $T(\tilde{\tau}_s)$ . Differencing these equations and with  $\tilde{\tau} = \tilde{\tau}_s$ ,

$$\sigma T_s^4 - \sigma T^4(\tilde{\tau}_s) = \frac{F_\infty}{2}.$$

The results of the model are presented in Fig. 4.6 a, showing the profiles of upward and downward fluxes and the profile of the temperature which is contained in the profile of flux  $\pi B$ . Highlighted are the skin temperatures, the discontinuity at the surface. At first sight, the model does not seem to bear any resemblance to the real temperature profile. This is because the coordinate  $\tau$  is not an easy coordinate to interpret. Let us suppose that  $\tau$  is largely defined by water vapor and that

$$\rho(\text{H}_2\text{O}) = \rho_0 e^{-z/H_{\omega}}$$

where  $H_{\omega} \approx 2 \text{ km}$ . To simplify matters, we assume that  $\tau$  varies with  $z$  in the same way  $\rho(\text{H}_2\text{O})$  varies with  $z$

$$\tau = \tau_s e^{-z/2} \quad (4.17)$$

and

$$\sigma T^4(z) = \frac{F_\infty}{2} \left[ 1 + \frac{3}{2} \tau^* e^{-z/2} \right]$$

The profile of temperature with height equivalent to Fig. 4.6a is presented in Fig. 4.6b. For comparison, the profile defined by a  $6 \text{ K km}^{-1}$  lapse rate is presented. We note that the radiative equilibrium profile is unstable throughout most of the atmosphere, at least to where the  $6 \text{ K km}^{-1}$  profile cuts the radiative equilibrium profile. This radiative equilibrium profile is unstable w.r.t. vertical motion and is destroyed by convection, which we may think of in this simple model as producing the constant lapse rate profile. Where the latter intersects the radiative equilibrium profile at about 10 km is where this simple model predicts the position of the tropopause.

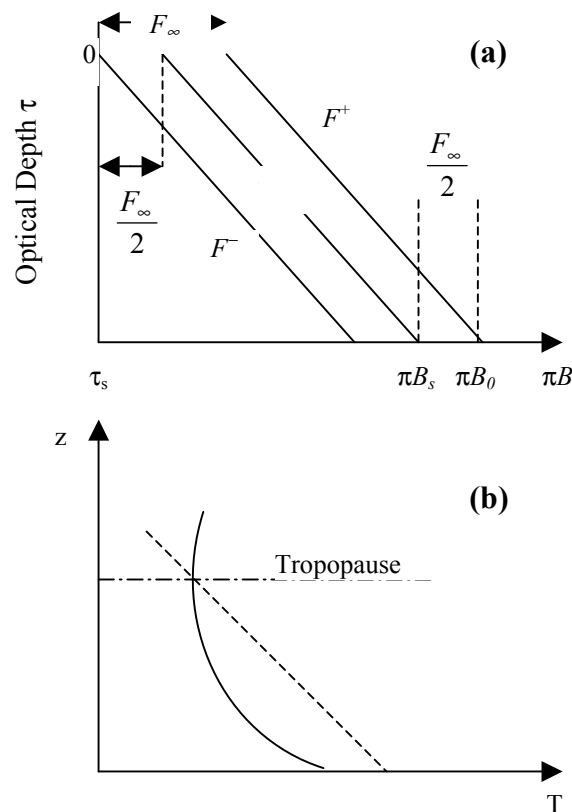


Fig. 4.6 (a) The flux profiles and black body function predicted by the simple gray body model as a function of optical depth. (b) The radiative equilibrium temperature profile as a function of altitude predicted by the flux model and assuming the profile of optical depth in Eqn. (4.17).

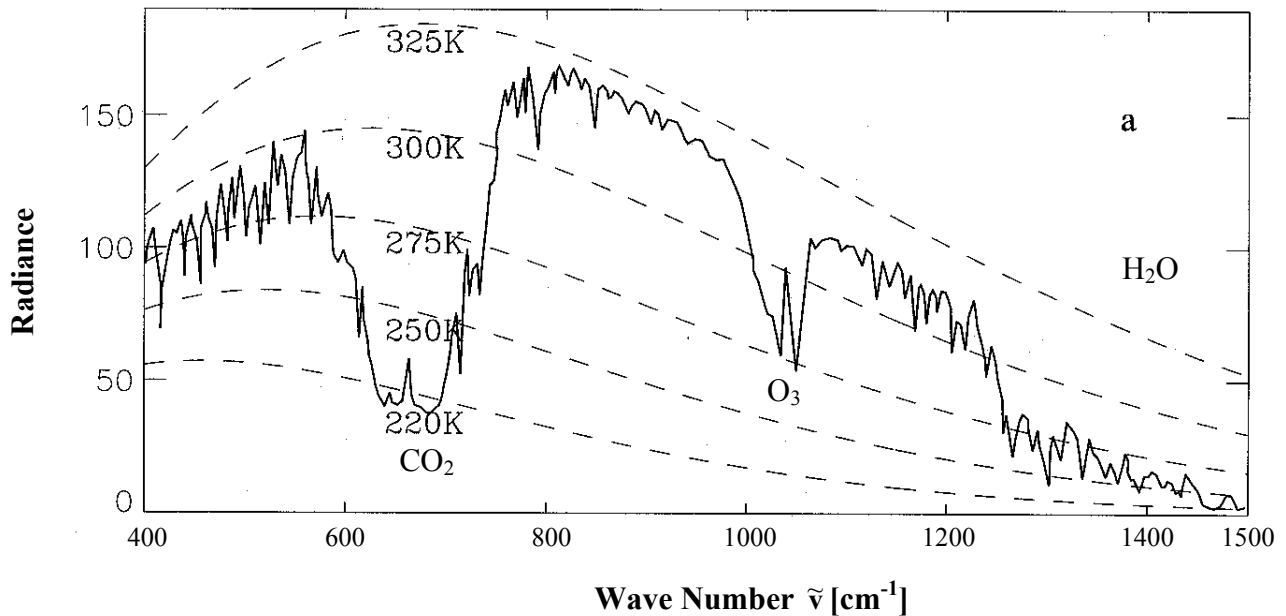
#### 4.6 Problems

The attached diagram presents the emission spectrum measured by an interferometer on a satellite viewing Earth.

- (1) Identify major absorption features in the spectrum.

- (2) What conditions (clear sky or cloudy, dry or moist atmosphere) do you think are applicable to measured spectrum?
- (3) Draw a schematic of the **difference** in the emission spectrum before and after a CO<sub>2</sub> doubling has occurred. Consider only clear sky conditions and the following two scenarios:
- CO<sub>2</sub> doubling with fixed absolute humidity
  - CO<sub>2</sub> doubling with fixed relative humidity

Briefly discuss the different spectra highlighting key features as they relate to a CO<sub>2</sub> increase (you may wish to draw these spectra as applied to global mean conditions).



*Earth's emission spectrum seen at the top of the atmosphere.*